

Secondary ion mass spectrometry induced damage adjacent to analysis craters in silicon

M. H. Clark and K. S. Jones^{a)}

Department of Material Science and Engineering, University of Florida, Gainesville, Florida 32611-6130

F. A. Stevie

Analytical Instrumentation Facility, North Carolina State University, Raleigh, North Carolina 27695

(Received 18 January 2002; accepted 3 June 2002)

Damage introduced by dynamic secondary ion mass spectrometry (SIMS) depth profiling is studied. A silicon sample with a boron marker layer was depth profiled by dynamic SIMS. After subsequent annealing at 750 °C for 30 min, the SIMS sample was reanalyzed by plan-view transmission electron microscope (PTEM) and SIMS. PTEM images showed the presence of interstitial defects near the original SIMS crater, and SIMS depth profiles of similar regions exhibited boron diffusivity enhancements. Excess interstitials were introduced into the Si surface up to 2 mm from the original 225 $\mu\text{m} \times 225 \mu\text{m}$ crater. Both PTEM and SIMS results showed that the damage and its effects diminished with an increase in distance from the original crater. © 2002 American Vacuum Society. [DOI: 10.1116/1.1497178]

I. INTRODUCTION

Dopant depth profiling with detection limits less than ppm while maintaining excellent depth resolution make dynamic secondary ion mass spectrometry (SIMS) indispensable for the development of semiconductor devices and their technological processes. In particular, high-density devices are commonly fabricated by a combination of low energy ion implantation and rapid thermal annealing processes to create very shallow junctions. SIMS characterization of the device structures as well as assessment of the processes used for fabrication is dependent upon limitations of the depth profiling.

Obtaining quantitatively accurate SIMS depth profiles for shallow junctions is complicated by the presence of ion implantation damage, precipitates and the pre-equilibrium region.¹ In addition, the SIMS depth profiling process itself introduces artifacts that can further complicate the analysis (e.g., mixing and/or redeposition).²

SIMS is based on the principle that charged atomic and molecular species are sputtered from the sample surface by ion bombardment. More specifically, the impact of the ions on the surface and their subsequent implantation causes an energy and momentum transfer to a limited area around the point of particle impact, resulting in a change in lattice structure and the sputtering of surface material.³ It is the change in lattice structure (i.e., damage) that is the culprit in most SIMS induced artifacts.

Fundamentally, the particle interactions occurring at the point of ion impact during SIMS are similar to those occurring during ion implantation. It follows then, that the damage produced by implantation of ions during SIMS analysis results in damage similar to that of ion implantation and can, therefore, produce similar phenomena. For example, ion implantation is notorious for producing interstitial defects,

which enhance the diffusivity of dopant implants such as boron upon thermal annealing.^{4,5} In light of this, repeated SIMS analyses after thermal processing may produce a SIMS diffusion artifact in subsequent dopant profiles.

The purpose of this study is to elucidate whether dynamic SIMS depth profiling does produce sufficient damage outside the intended analysis region and create interstitial defects, which in turn enhance the diffusion of boron upon subsequent thermal processing.

II. EXPERIMENT

A single SIMS depth profile was performed on a silicon wafer with a boron marker layer (i.e., boron spike) at a depth of approximately 4700 Å and peak concentration of $5.6 \times 10^{18} \text{ cm}^{-3}$. The wafer was constructed by epitaxially growing a buried boron marker layer and a subsequent undoped layer of silicon by chemical vapor deposition on a Czochralski grown *p*-type (100) silicon substrate. Dynamic SIMS analysis was carried out on a Cameca IMS-3f with a magnetic sector analyzer using an O_2^+ primary ion source, with a 5.5 keV impact energy, a 225 $\mu\text{m} \times 225 \mu\text{m}$ beam raster and a detected area 60 μm in diameter from the center of the crater.

Atomic force microscopy (AFM) was used to measure the surface roughness of the silicon wafer as a function of distance from the SIMS crater. AFM was performed by a Digital Instruments Nanoscope III scanning probe microscope in tapping mode with a silicon nitride (Si_3N_4) tip over a scan area of 1 $\mu\text{m} \times 1 \mu\text{m}$.

Following AFM analysis the sample was annealed in a tube furnace with a nitrogen ambient at 750 °C for 30 min. After annealing, three SIMS depth profiles were performed on the same silicon sample at increasing distances from the original crater to determine if the formation of the original SIMS crater had any effect on diffusion of the boron marker layer. The three postanneal depth profiles were taken at po-

^{a)}Electronic mail: kjoness@eng.ufl.edu

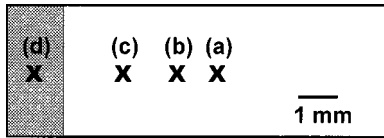


FIG. 1. Physical layout of the SIMS craters on the silicon sample in terms of distance from the center of the original SIMS crater: (a), (b) 1.0–1.2, (c) 1.8–2.0, and (d) >3.5 mm, shielded/no SIMS damage. The craters are not to scale.

sitions of increasing linear distance from the center of the original SIMS crater, with the third depth profile taken at a position that was shielded from bombardment during the original SIMS analysis (Fig. 1).

Based upon the postanneal SIMS depth profiles of the boron marker layer,⁶ the time average diffusivity enhancements of boron ($\langle D_B \rangle / D_B^*$) were calculated. To obtain the $\langle D_B \rangle / D_B^*$ values, the postanneal boron marker layer profiles were first normalized to the same depth and dose. Then the Florida Object Oriented Process Simulator (FLOOPS)⁷ was used to simulate the diffusion times necessary to match the enhanced diffusion of the boron marker layers. Finally, the $\langle D_B \rangle / D_B^*$ values were calculated from the ratio of the enhanced annealing times to the actual anneal times, which is directly proportional to the ratio of the experimentally observed diffusivity of boron ($\langle D_B \rangle$) to the intrinsic diffusivity of boron (D_B^*).

Transmission electron microscopy (TEM) was used to examine the possible damage introduced into the silicon sample by the dynamic SIMS process. TEM analysis was performed on a JEOL 200CX for both cross-sectional TEM (XTEM) and plan-view TEM (PTEM) samples.⁸ XTEM of regions in close proximity to the three postanneal SIMS craters was used to determine if the dynamic SIMS process amorphized the near crater surface region. XTEM images were taken in bright field on the [110] zone axis. Additionally, PTEM analysis of the original SIMS crater after annealing was used to observe any damage created by the dynamic SIMS process. PTEM images were taken using the g_{220} reflection and weak beam dark field (WBDF) conditions. Due to the destructive nature of TEM sample preparation, it was not possible to make both the XTEM and PTEM samples from the original silicon sample. Therefore, prior to any SIMS analysis a PTEM sample was prepared from the original silicon wafer and then subjected to the same experimental process, thus providing a second identical sample for PTEM analysis.

III. RESULTS AND DISCUSSION

Visual observation of the original SIMS crater revealed a halo/circle roughly 2 mm in diameter centered around the crater. In visual contrast the halo appeared bright whereas the surrounding material was dull. Initially, it was thought that the halo was formed by the sputtering of the native surface oxide during the dynamic SIMS process, however, the halo does not diminish over time (i.e., regrowth of native oxide), suggesting that it is due to surface modification other than

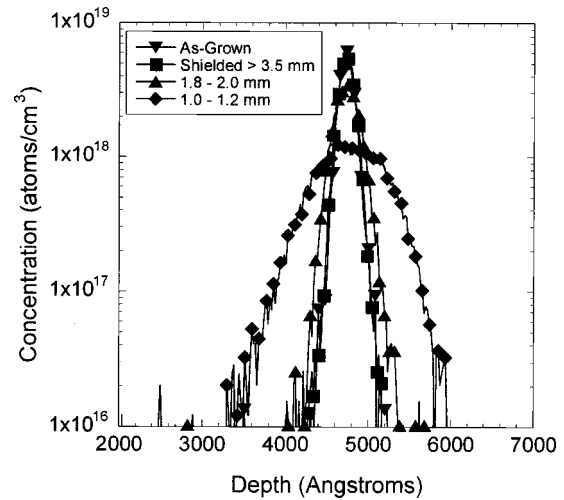


FIG. 2. SIMS depth profiles of the boron marker layer after annealing at 750 °C for 30 min, as a function of distance from the original SIMS crater.

removal of the native oxide. Furthermore, AFM analysis did not reveal any significant difference in the silicon sample's surface roughness, either inside or outside the halo, with an increase in distance from the original SIMS crater. In fact, surface roughness measurements of all regions yielded a value of approximately 5 Å, suggesting that the dynamic SIMS process was either not removing a detectable amount of the surface material beyond the crater itself or was removing the material gradually (i.e., a smooth gradient).

In preparation for the subsequent SIMS analysis, the original SIMS crater was annealed at 750 °C for 30 min. After annealing, no halo around the original SIMS crater could be discerned by visual observation. More specifically, the entire sample shared a uniform dull contrast. Lack of the halo after annealing suggests that the anneal was sufficient to recover/repair the modification that the process of dynamic SIMS had induced into the near crater region. If the halo were an amorphous region, its disappearance after annealing could be explained by solid phase epitaxial regrowth.

Figure 2 shows three SIMS depth profiles taken after the original SIMS crater had been annealed at 750 °C for 30 min. The plot illustrates that the farther away from the original SIMS crater the subsequent depth profiles are performed, the less diffusivity enhancement the boron marker layer experiences. The original SIMS depth profile performed before the anneal almost exactly matches that performed for the shielded area with the exception of a very small diffusivity enhancement, which is present for the shielded profile after the anneal.

Figure 3 shows the $\langle D_B \rangle / D_B^*$ experienced by the boron marker layer with respect to its relative proximity to the original SIMS crater. The plot shows that the $\langle D_B \rangle / D_B^*$ is reduced with an increase in distance from the original SIMS crater. Due to the interstitial nature of boron diffusion, there is a direct correlation between the $\langle D_B \rangle / D_B^*$ and the interstitial concentration (i.e., $\langle C_I \rangle / C_1^*$),^{5,9} thus suggesting that there is an increase in interstitial concentration with an increase in the proximity to the SIMS crater. As a point of

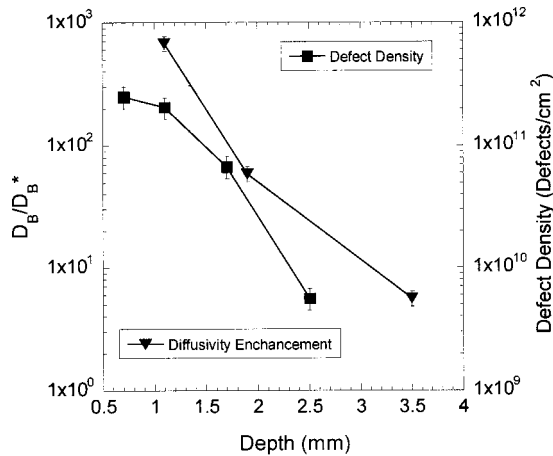


FIG. 3. Time average diffusivity enhancement and defect density as a function of distance from the original SIMS crater.

clarification, the $\langle D_B \rangle / D_B^*$ value calculated from the shielded depth profile is in agreement with other $\langle D_B \rangle / D_B^*$ values calculated for samples with no previous SIMS analysis after being annealed for the same time and temperature, thus demonstrating that the $\langle D_B \rangle / D_B^*$ value of 5 is intrinsic to the silicon wafer used in this study.

PTEM analysis of the area near the original SIMS crater revealed defects [Fig. 4(a)]. Defects observed by PTEM were similar to defects observed after low energy ion implantation and annealing.¹⁰ As in the case of ion implantation introduced defects, the defects observed by PTEM could provide a source of interstitials by which to drive the boron enhanced diffusivity.¹¹ The concentration of the defects observed by PTEM are displayed by the right hand ordinate axis in Fig. 3. It is apparent from Fig. 3 that with an increase in distance from the original SIMS crater the defect population drops off. The reduction in the defect population is consistent with the diffusivity enhancement results and lends credibility to the assertion that the defects are the source of interstitials.

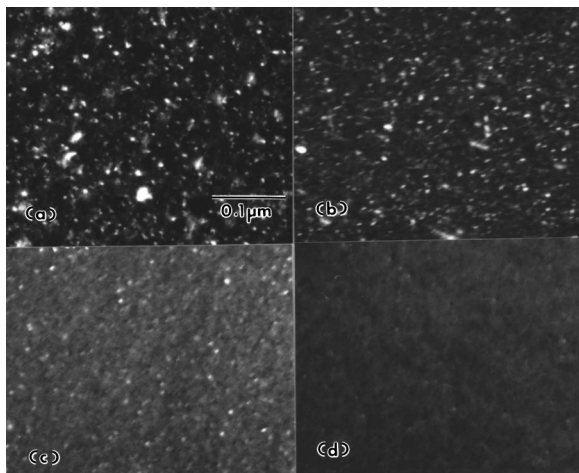


FIG. 4. WDF g_{220} plan-view transmission electron micrographs of the damage created by a SIMS depth profile after annealing at 750 °C for 30 min, at distances of (a) 0.6–0.8, (b) 1.0–1.2, (c) 1.4–1.6, and (d) 1.8–2.0 mm from the original SIMS crater.

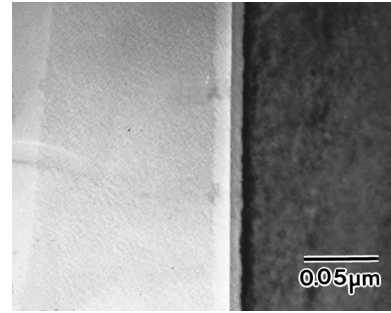


FIG. 5. Bright-Field XTEM micrograph of the amorphous layer created by SIMS depth profiling. The amorphous layer is 78 Å thick and is shown as the light-gray region bordering the rough dark band.

Ion implantation damage provides a reasonable explanation for both the halo and the enhanced diffusivity of the boron marker layer. The enhanced diffusivity of the boron marker layers observed by SIMS is indicative of damage introduced into the sample by means of ion implantation,¹² as explained by the interaction of boron and interstitials. Ion implantation damage of the near crater region also provides a reasonable explanation for the halo. If the halo were an amorphous region, then a 30 min 750 °C would result in solid phase epitaxy regrowth of the region and leave no sign of the original amorphous halo. Additionally, the lack of surface roughening observed by AFM is consistent with the formation of an amorphous layer. Confirming the indications of an amorphous region, XTEM of the halo region, prior to annealing, shows an amorphous layer approximately 78 Å in depth (Fig. 5).

Damage created by SIMS depth profiling most likely occurs from either the Gaussian nature of the ion beam or neutrals. Since the ion beam has a Gaussian tail, a small number of ions bombard the sample outside the crater region creating ion implantation damage; however, given the exponential decrease in the tail, this contribution is expected to diminish quickly with an increase in distance from the crater. Therefore, at a distance of 2 mm from the crater it is doubtful that the tail would be able to introduce damage above a detectable limit (i.e., $1E-13$ interstitials/cm²).¹³ On the other hand, neutrals generated in the ion beam cannot be focused/controlled by the system optics and thus bombard the sample over a much larger area than the crater. Neutrals as the source of damage is further supported by the fact that the Cameca IMS-3f has no bend in the beam line to prevent neutrals from hitting the surface of the sample.

IV. CONCLUSIONS

SIMS depth profiling introduced implantation damage into the silicon sample outside the analysis crater. Damage created by SIMS depth profiling was detectable after a 750 °C, 30 min anneal by both PTEM and subsequent SIMS analysis for a distance up to 2 mm from the original crater. As measured by both SIMS and PTEM, the damage introduced into the silicon sample is a function of the proximity to the original SIMS crater, thus the closer to the crater the

larger the damage and diffusivity enhancement. The results suggest that the damage is produced by neutrals in the ion beam. These findings indicate that SIMS analysis needs to be done with caution and with awareness of processes that may produce deleterious artifacts.

ACKNOWLEDGMENTS

The AFM work was performed by Loren Rieth at the University of Florida. The authors thank the University of Central Florida for use of their Cameca IMS-3f.

¹E. A. Clark, M. G. Dowsett, H. S. Fox, and S. M. Newstead, *High Precision Depth Profiling of Implanted Semiconductors* (Wiley, New York, 1989), pp. 627–630.

²V. K. F. Chia, in *Materials and Process Characterization of Ion Implantation*, 1st ed., edited by M. I. Current and C. B. Yarling (Ion Beam Press, Austin, 1997), pp. 163–200.

³A. Benninghoven, F. G. Rudenauer, and H. W. Werner, *Secondary Ion Mass Spectrometry; Basic Concepts, Instrumental Aspects, Applications and Trends* (Wiley, New York, 1987), Vol. 86.

⁴P. A. Packan and J. D. Plummer, *Appl. Phys. Lett.* **56**, 1787 (1990).

⁵P. A. Packan, Ph.D. thesis, Stanford University, Stanford, CA, 1991.

⁶H. J. Gossmann, C. S. Rafferty, A. M. Vredenberg, H. S. Luftman, F. C. Unterwald, D. J. Eaglesham, D. C. Jacobson, T. Boone, and J. M. Poate, *Appl. Phys. Lett.* **64**, 312 (1993).

⁷M. E. Law, G. H. Gilmer, and M. Jaraiz, *MRS Bull.* **45** (2000).

⁸K. S. Jones, Ph.D. thesis, University of California, 1987.

⁹H.-J. Gossmann, G. H. Gilmer, C. S. Rafferty, F. C. Unterwald, T. Boone, and J. M. Poate, *J. Appl. Phys.* **77**, 1948 (1995).

¹⁰D. F. Downey and K. S. Jones, in *The Role of Extended Defects on the Formation of Ultra-shallow Junctions in Ion Implanted 11B+, 49BF2, 75As+ and 31P+*, Kyoto, Japan, 1998, pp. 897–901.

¹¹D. J. Eaglesham, P. A. Stolk, H.-J. Gossmann, and J. M. Poate, *Appl. Phys. Lett.* **65**, 2305 (1994).

¹²Y. Kim, H. Z. Masoud, and R. B. Fair, *J. Electron. Mater.* **18**, 143 (1988).

¹³D. J. Eaglesham, P. A. Stolk, H.-J. Gossmann, T. E. Haynes, and J. M. Poate, *Nucl. Instrum. Methods Phys. Res. B* **106**, 191 (1995).